

# Resonant photoemission spectroscopy study of insulator-to-metal transition in Cr- and Ru-doped $\text{Nd}_{1/2}\text{A}_{1/2}\text{Mn}_{1-y}\text{O}_3$ ( $\text{A}=\text{Ca}, \text{Sr}$ )

J. -S. Kang<sup>1</sup>, J. H. Kim<sup>1</sup>, A. Sekiyama<sup>2</sup>, S. Kasai<sup>2</sup>, S. Suga<sup>2</sup>, S. W. Han<sup>3</sup>, K. H. Kim<sup>3</sup>, E. J. Choi<sup>4</sup>, T. Kimura<sup>5</sup>, T. Muro<sup>6</sup>, Y. Saitoh<sup>7</sup>, C. G. Olson<sup>8</sup>, J. H. Shim<sup>9</sup>, and B. I. Min<sup>9</sup>

<sup>1</sup>Department of Physics, The Catholic University of Korea, Puchon 420-743, Korea

<sup>2</sup>Department of Material Physics, Graduate School of Engineering Science, Osaka University, Osaka 560-8531, Japan

<sup>3</sup>Department of Physics, Gyeongsang National University, Chinju 660-701, Korea

<sup>4</sup>Department of Physics, The University of Seoul, Seoul 130-743, Korea

<sup>5</sup>Department of Applied Physics, University of Tokyo, Tokyo 113-0033, Japan

<sup>6</sup>Japan Synchrotron Radiation Research Institute (JASRI), SPring-8, Hyogo 679-5198, Japan

<sup>7</sup>Department of Synchrotron Radiation Research, Kansai Research Establishment, Japan Atomic Energy Research Institute (JAERI), SPring-8, Hyogo 679-5148, Japan

<sup>8</sup>Korea Research Institute of Standards and Science, Taejeon 305-600, Korea

<sup>9</sup>Ames Laboratory, Iowa State University, Ames, Iowa 50011, U.S.A.

<sup>9</sup>Department of Physics, Pohang University of Science and Technology, Pohang 790-784, Korea  
(February 1, 2008)

Electronic structures of very dilute Cr- or Ru-doped  $\text{Nd}_{1/2}\text{A}_{1/2}\text{MnO}_3$  (NAMO;  $\text{A}=\text{Ca}, \text{Sr}$ ) manganites have been investigated using the Mn and Cr  $2p \rightarrow 3d$  resonant photoemission spectroscopy (PES). All the Cr- and Ru-doped NAMO systems exhibit the clear metallic Fermi edges in the Mn  $e_g$  spectra near  $E_F$ , consistent with their metallic ground states. The Cr  $3d$  states with  $t_{2g}^3$  configuration are at  $\sim 1.3$  eV below  $E_F$ , and the Cr  $e_g$  states do not participate in the formation of the band near  $E_F$ . Cr- and Ru-induced ferromagnetism and insulator-to-metal transitions can be understood with their measured electronic structures.

PACS numbers: 79.60.-i, 75.47.Lx, 71.30.+h

The Mn-site doping by magnetic cations, such as Cr, Ru, is known to be a very efficient method to induce metallicity and ferromagnetism in the insulating and antiferromagnetic (AFM)  $\text{Nd}_{1/2}\text{A}_{1/2}\text{MnO}_3$  (NAMO;  $\text{A}=\text{Ca}, \text{Sr}$ ) [1,2,3,4]. Undoped NAMO has the charge/orbital ordered (CO/OO) insulating phase with the CE-type AFM spin ordering. By doping Ru to NAMO, the Curie temperature  $T_C$  is even enhanced [5]. To explain the Cr-induced insulator-to-metal (I-M) transition, the relaxor-ferromagnet has been proposed [4], in which the field-induced I-M transition takes place due to the growth of ferromagnetic microclusters in a matrix of CO/OO state. On the other hand, two valence states of Ru ions are proposed to explain the Ru-induced ferromagnetism [6]. However, these proposals have not been proved yet and the different behavior of Cr and Ru doping is not well understood.

To explore the melting mechanism of CO/OO in these systems, the main issues to be resolved are: (i) the valence and spin states of impurities and (ii) the role of impurities in the metallic band formation. Photoemission spectroscopy (PES) provides direct information on the electronic structures of the CO manganites [7,8]. In this paper, we report the *bulk-sensitive* [9] high-resolution valence-band photoemission spectroscopy (PES) study for Cr- and Ru-doped NAMO manganites, including resonant photoemission spectroscopy (RPES) [8,9,10] near the Mn and Cr  $2p$  and Nd  $4d$  and  $3d$  absorption edges. Using the large resonance enhancement in the  $2p \rightarrow 3d$  RPES [8], we were able to measure clearly

the Cr  $3d$  emission for a very dilute Cr-doped system:  $\text{Nd}_{1/2}\text{A}_{1/2}\text{Mn}_{1-y}\text{Cr}_y\text{O}_3$  ( $\text{A}=\text{Ca}, \text{Sr}$ ;  $y=0.05, 0.07$ ), corresponding to only  $\sim 1$  atomic %. Therefore this work opens up the possibility of directly observing the local electronic structure of very dilute transition-metal systems. Furthermore, our PES measurements for a wide photon energy ( $h\nu$ ) range ( $h\nu \approx 20$  eV – 1000 eV) allow us to determine various partial spectral weight distributions (PSWs) by using the cross-section effect over a wide  $h\nu$  range. We have also made a comparison with the Ru-doped  $\text{Nd}_{1/2}\text{Sr}_{1/2}\text{Mn}_{1-y}\text{Ru}_y\text{O}_3$  ( $y=0.05$ ).

$\text{Nd}_{1/2}\text{A}_{1/2}\text{Mn}_{1-y}\text{T}_y\text{O}_3$  single crystals ( $\text{A}=\text{Ca}, \text{Sr}$ ;  $\text{T}=\text{Cr}, \text{Ru}$ ;  $0 \leq y \leq 0.1$ ) were grown using the floating zone method. The details of the crystal growing method is described elsewhere [4]. High-resolution T  $2p \rightarrow 3d$  RPES ( $\text{T}=\text{Cr}, \text{Mn}$ ) experiments were performed at the twin-helical undulator beam line BL25SU of SPring-8 equipped with a SCIENTA SES200 analyzer [11]. Samples were fractured and measured in vacuum better than  $3 \times 10^{-10}$  Torr at  $T \lesssim 20$  K. PES data were obtained in the transmission mode, with the overall energy resolution [FWHM : full width at half maximum] of about 80 meV at  $h\nu \sim 600$  eV. All the spectra were normalized to the photon flux estimated from the mirror current. Low energy PES experiments were carried out at the Ames/Montana beamline at the Synchrotron Radiation Center (SRC). Samples were fractured and measured in vacuum with a base pressure better than  $3 \times 10^{-11}$  Torr and at  $T \lesssim 15$  K with the FWHM  $\approx 80$  meV at  $h\nu \approx 20$  eV. The fractured surfaces were rough and the measured

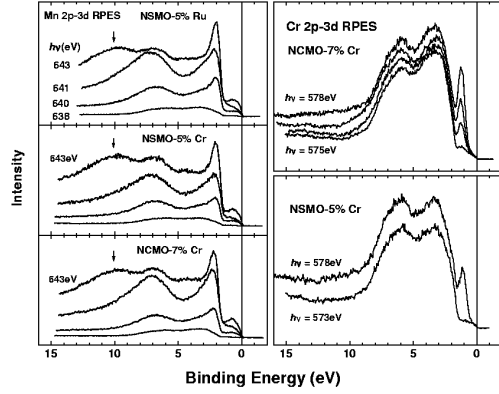


FIG. 1. Left: The Mn  $2p \rightarrow 3d$  RPES spectra of NSMO-5%Ru, NSMO-5%Cr, and NCMO-7%Cr around  $h\nu \sim 640$  eV. The bump structures below the arrow are due to the Mn LMM Auger emission. Right: The Cr  $2p \rightarrow 3d$  RPES spectra of NCMO-7%Cr and NSMO-5%Cr around  $h\nu \sim 575$  eV.

spectra showed no angle-dependence, suggesting that our PES data could be considered as being angle-integrated. All the samples showed a clean single peak in the O  $1s$  core-level spectra and no 9 eV binding energy (BE) peak in the valence-band spectra.

Figure 1 shows the valence-band spectra of Cr- and Ru-doped  $\text{Nd}_{1/2}\text{Ca}_{1/2}\text{MnO}_3$  (NCMO) and  $\text{Nd}_{1/2}\text{Sr}_{1/2}\text{MnO}_3$  (NSMO) near the Mn and Cr  $2p_{3/2}$  absorption edges. Large enhancement is observed across the Mn ( $h\nu = 643$  eV) and Cr ( $h\nu = 578$  eV) absorption edges. Our Mn  $2p \rightarrow 3d$  RPES spectra for Cr- and Ru-doped NCMO and NSMO are similar to those of the previous report on CO NSMO [8]. As to the resonating behavior of the Mn  $3d$ -derived states (the left panel), those near  $\sim 2.3$  eV BE and  $E_F$  ( $0 \sim 1$  eV) are identified as the  $t_{2g}^3$  and  $e_g^x$  ( $x \approx 0.5$ ) majority-spin states, respectively. These RPES measurements reveal that the high BE features ( $5 \sim 8$  eV) also have the large Mn  $3d$  electron character, which is strongly hybridized with the O  $2p$  electrons. The broad bump around 10 eV BE (denoted by arrow) for  $h\nu \sim 643$  eV is due to the Mn LMM Auger emission.

In the right panel, the sharp resonating feature around  $\sim 1.3$  eV BE indicates strong Cr  $3d$  character. The absence of the Cr  $3d$  electron emission near  $E_F$  indicates that doped Cr ions in NCMO and NSMO are in the localized trivalent  $\text{Cr}^{3+}$  states ( $t_{2g}^3$  configuration), and that Cr  $e_g$  states are located above the Mn  $e_g$  states. In fact, our Cr  $2p$  XAS spectrum of NCMO (not shown here) is very similar to that of a formally trivalent  $\text{Cr}_2\text{O}_3$  [12], but quite different from those of formally divalent or tetravalent Cr compounds. It thus suggests that Cr  $e_g$  states do not participate in the formation of the band near  $E_F$ , nor affect the bandwidth of the  $e_g$  states near  $E_F$ . This feature can be understood based on the previous finding that Cr spins order antiparallel to the Mn subnetwork

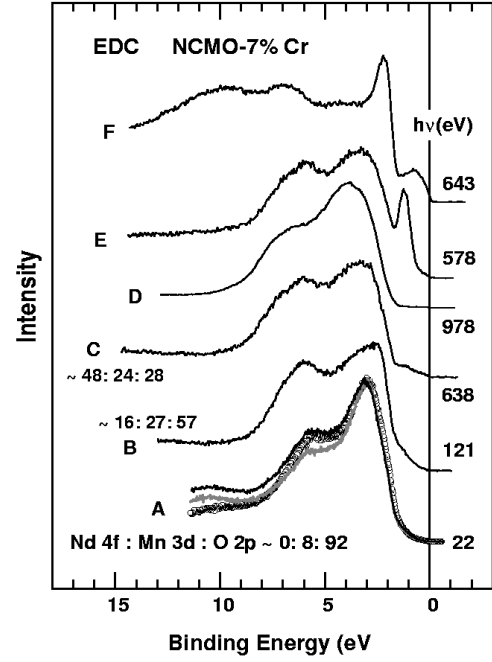


FIG. 2. Valence-band spectra of NCMO-7%Cr for a wide  $h\nu$  range ( $22 \text{ eV} \leq h\nu \leq 978 \text{ eV}$ ). The  $h\nu = 978$  eV spectrum is that for NSMO-5% Ru, which is essentially the same as for NCMO-7%Cr. See Ref. [15] for the details.

[13], and so the hopping between Cr and neighboring Mn ions is not allowed. This conclusion is supported by the comparison of the  $e_g$  spectra near  $E_F$  in Fig. 3.

Figure 2 compares the valence-band spectra of 7% Cr-doped NCMO for a wide  $h\nu$  range ( $22 \text{ eV} \leq h\nu \leq 978 \text{ eV}$ ). The different valence-band line shapes with varying  $h\nu$  reflect different contributions from different electron character. Note that these high- $h\nu$  PES spectra can be considered to represent the bulk electronic states [9,14]. The top three spectra represent the on-resonance spectra in the Mn  $2p \rightarrow 3d$ , Cr  $2p \rightarrow 3d$ , and Nd  $3d \rightarrow 4f$  RPES. Therefore the enhanced features in the top three spectra are due to the Mn  $3d$ , Cr  $3d$ , and Nd  $4f$  electron emissions. The resonance enhancement for the Nd  $3d \rightarrow 4f$  RPES is so large that the on-resonance spectrum ( $h\nu = 978$  eV) can be considered as the Nd  $4f$  partial spectral weight (PSW) [15].

If one assumes  $\text{Nd}^{3+}$  ( $4f^3$ ),  $\text{Mn}^{3.5+}$  ( $3d^3 - 3d^4$ ), and the filled O  $2p$  bands ( $2p^6$ ) in NCMO, and ignores the resonance effect, then the cross-section ratio of Nd  $4f$  : Mn/Cr  $3d$  : O  $2p$  electrons per unit cell is about  $\sim 1\%$  :  $\sim 8\%$  :  $\sim 92\%$  at  $h\nu \approx 22$  eV,  $\sim 16\%$  :  $\sim 27\%$  :  $\sim 57\%$  at  $h\nu \approx 120$  eV, and  $\sim 48\%$  :  $\sim 24\%$  :  $\sim 28\%$  at  $h\nu \approx 640$  eV [16]. Therefore the  $h\nu = 22$  eV spectrum can be considered as the O  $2p$  PSW. In the the  $h\nu = 22$  eV spectra, open circles and gray lines denote that for 2% Cr-doped NSMO and 4% Cr-doped NCMO, respectively. The similar lineshapes at  $h\nu = 22$  eV indicate that the O

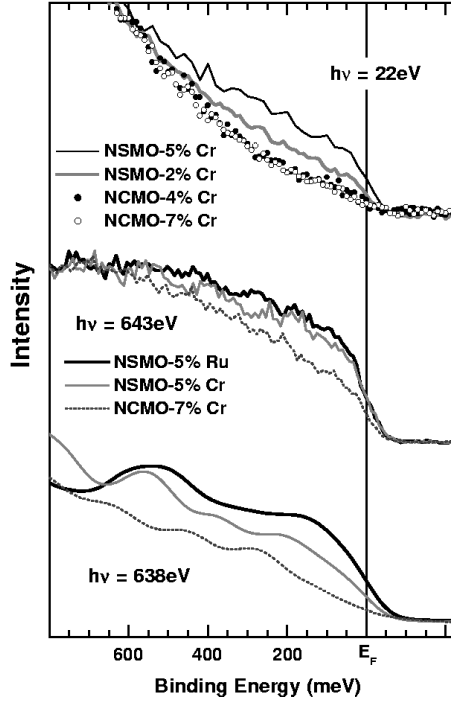


FIG. 3. Near- $E_F$  region of the valence-band spectra of  $\text{Nd}_{1/2}\text{A}_{1/2}\text{Mn}_{1-y}\text{T}_y\text{O}_3$  ( $\text{A}=\text{Ca}, \text{Sr}$ ;  $\text{T}=\text{Cr}, \text{Ru}$ ) at  $h\nu = 22$  eV (top) and at the  $\text{Mn } 2p \rightarrow 3d$  on-resonance ( $h\nu \approx 643$  eV) (middle). These spectra were obtained with  $\sim 80$  meV at FWHM. Bottom: the Near- $E_F$  spectra at the  $\text{Mn } 2p \rightarrow 3d$  off-resonance ( $h\nu \approx 638$  eV), obtained with  $\sim 150$  meV at FWHM.

$2p$  states are very similar in Cr-doped NAMO manganites. As  $h\nu$  increases, the  $\text{Mn } 3d$  and  $\text{Nd } 4f$  emissions increase with respect to the  $\text{O } 2p$  emission, and the  $\text{Mn } 3d$  and  $\text{O } 2p$  emissions become comparable to each other at  $h\nu \approx 638$  eV (the  $\text{Mn } 2p \rightarrow 3d$  off-resonance). In fact, we have observed that the overall features of Cr- and Ru-doped NAMO ( $\text{A}=\text{Ca}, \text{Sr}$ ) are very similar at  $h\nu = 638$  eV, and that the valence-band widths for NCMO systems are slightly narrower than those for NSMO systems [17], which is consistent with the larger ionic size of Sr than for Ca, causing the electron hopping easier.

The  $\text{Nd } 4f$ -derived states exhibit two broad peaks around  $\sim 4$  eV and  $\sim 7$  eV BE, which overlap substantially with the  $\text{O } 2p$  states between 3 – 6 eV (see the  $h\nu = 22$  eV spectrum). No emission is observed near  $E_F$  where the  $\text{Mn } e_g$  bands are located. These observations suggest that  $\text{Nd } 4f$  states are strongly hybridized with the  $\text{O } 2p$  states, but very little with the  $\text{Mn } e_g$  states. Thus the  $\text{Nd } 4f$  states do not participate in the band formation near  $E_F$ . We have found [17] that the  $\text{Nd } 4f$  PSWs of Cr- and Ru-doped NAMO ( $\text{A}=\text{Ca}, \text{Sr}$ ), determined from the  $\text{Nd } 4d \rightarrow 4f$  RPES, are essentially the same as one another and also very similar to that determined from the  $\text{Nd } 3d \rightarrow 4f$  RPES. Considering the

difference in the electron mean free paths between the  $\text{Nd } 4d \rightarrow 4f$  RPES and the  $\text{Nd } 3d \rightarrow 4f$  RPES, this finding indicates that the *surface*  $\text{Nd } 4f$  states are very similar to the *bulk*  $\text{Nd } 4f$  states in NAMO manganites, which makes a sharp contrast to the case of Ce compounds [14]. We interpret the  $\text{Nd } 4f$  PSW to represent roughly the  $4f^3$  ground state, but with the large final-state hybridization to  $\text{O } 2p$  orbitals [10,18].

Figure 3 compares the near- $E_F$  regions of the valence-band spectra of Cr- or Ru-doped NCMO and NSMO at  $h\nu = 22$  eV (top), and at the on-resonance energy of the  $\text{Mn } 2p \rightarrow 3d$  RPES ( $h\nu \approx 643$  eV) (middle). The  $h\nu \approx 643$  eV spectra (middle) correspond to the  $\text{Mn } e_g$  PSWs. At  $h\nu \approx 643$  eV, the metallic Fermi edges are clearly observed for all the samples, which is consistent with their metallic ground states. In contrast, the spectral intensity near  $E_F$  ( $I(E_F)$ ) in the  $h\nu = 22$  eV is very weak in view of the metallic nature of the samples. This difference arises from the fact the  $\text{O } 2p$  emissions are dominant at  $h\nu = 22$  eV and that the  $\text{O } p$  states have a negligible contribution near  $E_F$ . This comparison reveals that  $\text{Mn } e_g$  states play an important role in determining the I-M transition. For comparison, the spectra at the off-resonance energy of the  $\text{Mn } 2p \rightarrow 3d$  RPES ( $h\nu \approx 638$  eV) are shown at the bottom, which were obtained with a lower resolution (FWHM  $\sim 130$  meV) than the above spectra (FWHM  $\sim 80$  meV) [19]. For all the cases,  $I(E_F)$  is lower for the NCMO-based system than for the NSMO-based system, reflecting the stronger metallic nature for NSMO than for NCMO. Note that the larger Cr-doped NSMO exhibits a higher  $I(E_F)$  than the smaller Cr-doped NSMO (see  $h\nu = 22$  eV), and that the Ru-doped NSMO shows a higher  $I(E_F)$  than the Cr-doped NSMO (see  $h\nu = 638$  eV). These features are consistent with the observations that the metallic nature increases with the higher Cr-doping and that  $T_C$  is higher for the Ru-doped NSMO than for the Cr-doped NSMO.

Now let us discuss the melting mechanism in Cr- and Ru-doped NAMO, based on our observations. The undoped CO/OO NAMO is expected to have the ordered  $\text{Mn}^{3+}/\text{Mn}^{4+}$  ( $3d^4/3d^3$ ) configuration with the CE-type AFM spin ordering. We have found that Cr  $t_{2g}$  states are located well below  $E_F$ , resulting in the trivalent  $\text{Cr}^{3+}$  state ( $d^3$ ), as shown in the schematic diagram for the local density of states (Fig. 4). Then the substitution of a  $\text{Cr}^{3+}$  ( $d^3$ ) for a  $\text{Mn}^{3+}$  ( $d^4$ ) site in the CO/OO NAMO will correspond to the hole filling in the undoped NAMO, and it will play a role similar to the substitution of a  $\text{Mn}^{4+}$  ion for a  $\text{Mn}^{3+}$  ion. So one can simply conjecture that the CO/OO insulating phase is transformed into the metallic phase by breaking the commensurate quarter filling state. For example, the phase diagram of NSMO manifests that, with increasing the hole concentration, the CO/OO insulating phase of half-doped NSMO with the CE-type AFM is transformed into the metallic A-type AFM [20,21]. Similarly, one can also infer that the substitution of  $\text{Ru}^{4+}$  ( $d^4$ ) into a  $\text{Mn}^{4+}$  ( $d^3$ ) site will correspond to the electron filling, and so the CO/OO insulat-

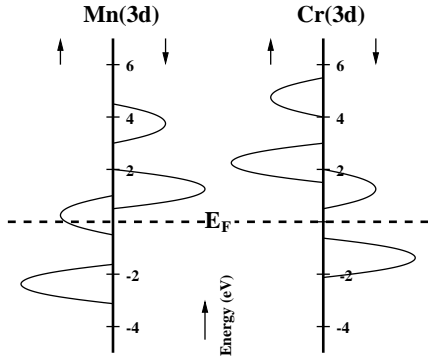


FIG. 4. Schematic local density of states of Mn and Cr for Cr-doped NAMO.

ing phase of half-doped NSMO is transformed into the metallic ferromagnetic phase.

The above picture of the filling control, however, is not complete since Cr-doped NSMO is not A-type AFM but ferromagnetic. Moreover, the stronger CO system NCMO would not exhibit the metallic phase merely with the filling control. It is thus likely that, not just the valence state but also other characteristics such as the spin state and the electronic structure are important. The localized spin of  $\text{Cr}^{3+}$  affects the spin ordering. The AFM superexchange interaction between  $\text{Cr}^{3+}$  and neighboring  $\text{Mn}^{4+}$  ions will give rise to the so-called *domino effect* of reversing the spin directions of  $\text{Mn}^{3+}/\text{Mn}^{4+}$  in the ferromagnetic zig-zag chain of the CE-type AFM [6]. Likewise, the FM superexchange interaction between  $\text{Ru}^{4+}$  and neighboring  $\text{Mn}^{3+}$  ions also gives rise to the domino effect of reversing the spin directions of  $\text{Mn}^{3+}/\text{Mn}^{4+}$ . In addition, since  $\text{Cr}^{3+}$  is not a Jahn-Teller active ion, it will play as a defect for the OO and the hopping strength will be enhanced around Cr ions due to the reduced Jahn-Teller polaron narrowing effect. Hence, the metallic phase could be formed even in NCMO at least around Cr ions, albeit not in whole crystal, if the double-exchange (DE) hopping strength becomes larger than the AFM superexchange interaction [20,21] or the hopping strength is larger than the intersite Coulomb interaction between carriers [22]. This picture is consistent with the concept of relaxor-ferromagnet [4]. Note that, in the metallic phase,  $\text{Cr}^{3+}$  itself does not participate in the DE mechanism because two configurations of  $\text{Mn}^{3+}-\text{Cr}^{3+}$  and  $\text{Mn}^{4+}-\text{Cr}^{2+}$  are not degenerate, as observed in the PES above. That is, doped  $\text{Cr}^{3+}$  would just play a role of initiating the hopping of carriers in the system.

To summarize, the electronic structures of very dilute Cr- and Ru-doped NAMO have been investigated by employing RPES. The large resonance enhancement in the  $2p \rightarrow 3d$  RPES allows us to observe clearly the Cr  $3d$  emission in very dilute ( $\sim 1$  atomic %) Cr-doped NAMO. The Cr  $3d$  states are observed at  $\sim 1.3$  eV below  $E_F$ , cor-

responding to the  $t_{2g}^3$  configuration of  $\text{Cr}^{3+}$  ions. This finding suggests that Cr  $e_g$  states are located above the Mn  $e_g$  states and they do not participate in the formation of the band near  $E_F$ . All the Cr- and Ru-doped NAMO systems exhibit the clear metallic Fermi edges in the Mn  $e_g$  spectra near  $E_F$ , consistent with their metallic ground states. The spectral intensity at  $E_F$  is higher for the NSMO-based system than for the NCMO-based system, reflecting the stronger metallic nature for NSMO than for NCMO because of the larger ionic size of Sr than for Ca. Further, Ru-doped NSMO has higher spectral intensity near  $E_F$  than Cr-doped NSMO, consistent with a higher  $T_C$  for Ru-doped NSMO.

**Acknowledgments**— This work was supported by the KRF (KRF-2002-070-C00038) and the KOSEF through the CSCMR at SNU and the eSSC at POSTECH. PES experiments were performed at the SPring-8 (JASRI: 2001B0028-NS-np) and at the SRC (NSF: DMR-0084402).

- 
- [1] B. Raveau, A. Maignan, and C. Martin, *J. Solid State Chem.* **130**, 162 (1997).
  - [2] A. Barnabé *et al.*, *Appl. Phys. Lett.* **71**, 3907 (1997).
  - [3] Y. Moritomo *et al.*, *Phys. Rev. B* **60**, 9220 (1999).
  - [4] T. Kimura *et al.*, *Phys. Rev. Lett.* **83**, 3940 (1999); *Phys. Rev. B* **62**, 15021 (2000).
  - [5] A. Maignan *et al.*, *J. Appl. Phys.* **89**, 500 (2001).
  - [6] C. Martin *et al.*, *Phys. Rev. B* **63**, 174402 (2001).
  - [7] A. Chainani *et al.*, *Phys. Rev. B* **56**, R15513 (1997).
  - [8] A. Sekiyama *et al.*, *Phys. Rev. B* **59**, 15528 (1999).
  - [9] J.-S. Kang *et al.*, *Phys. Rev. B* **66**, 113105 (2002).
  - [10] S. Suga *et al.*, *Phys. Rev. B* **52**, 1584 (1995).
  - [11] Y. Saitoh, *et al.*, *Rev. Sci. Instrum.* **71**, 3254 (2000).
  - [12] C. Theil *et al.*, *Phys. Rev. B* **59**, 7931 (1999).
  - [13] O. Toulemonde *et al.*, *J. Appl. Phys.* **86**, 2616 (1999).
  - [14] A. Sekiyama *et al.*, *Nature (London)* **403**, 398 (2000).
  - [15] The  $h\nu = 978$  eV spectrum in Fig. 2 is that of NSMO-5% Ru because we do not have that spectrum for NCMO-7% Cr. However, we have found [17] that the Nd  $4f$  PSW is essentially the same for Cr- and Ru-doped NCMO and NSMO.
  - [16] J.J. Yeh and I. Lindau, *At. Data Nucl. Data Tables* **32**, 1 (1985).
  - [17] J.-S. Kang *et al.*, unpublished (2002).
  - [18] J. -S. Kang *et al.*, *Phys. Rev. B* **60**, 13257 (1999).
  - [19] The off-resonance spectra shown at the bottom have been smoothed by using a Gaussian function of 100 meV at FWHM to reduce the signal-to-noise ratio. However, the trend observed in the raw spectra is still maintained.
  - [20] J. van den Brink and D. Khomskii, *Phys. Rev. Lett.* **82**, 1016 (1999).
  - [21] B. I. Min, Y.-K. Jo, M.-S. Kim, *Physica B* **312**, 723 (2002).
  - [22] J. D. Lee and B. I. Min, *Phys. Rev. B* **55**, R14713 (1997)